Cell Biochemistry and Biophysics (2025) 83:2115–2126
https://doi.org/10.1007/s12013-024-01621-1

ORIGINAL PAPER

Studies on the Role of MAP4K2, SPI1, and CTSD in Osteoporosis

Chao Sun[1,2] · Wanxiong He[2] · Leipeng Wang[1,2] · Ting Hao[1,2] · Xiaolong Yang[1,2] · Wei Feng[1,2] · Yonggang Wu[3] · Chenyang Meng[1,2] · Zhi Wang[3] · Xiaofeng Chen[1,2] · Mingqi Sun[1,2] · Feng Zheng[4] · Baoxin Zhang[1,2,5]

Accepted: 10 November 2024 / Published online: 25 November 2024
© The Author(s) 2024

Abstract

Osteoporosis (OP) is a prevalent skeletal disorder characterized by an imbalance between bone resorption and bone formation, resulting in a significant global burden. Previous research utilizing bioinformatics analysis has identified MAP4K2, SPI1, and CTSD as hub genes associated with OP. In this current investigation, we have successfully established a differential expression system of MAP4K2, SPI1, and CTSD in rat bone marrow mesenchymal stem cells (BMSCs) through transfection techniques. Additionally, the CCK-8 assay was employed to assess cell proliferation, while the alkaline phosphatase (ALP) activity assay and ALP staining assay were utilized to evaluate osteogenic differentiation. Alizarin red staining was employed to detect mineralization of BMSCs. Furthermore, the expression of relevant genes and molecules associated with the MAPK signaling pathway, autophagy, and apoptosis in the sera of rat BMSCs were examined using quantitative real-time polymerase chain reaction (qRT-PCR). The purpose of this study was to preliminarily investigate whether MAP4K2, SPI1, and CTSD have an effect on the osteogenic capacity of rat BMSCs and whether these genes, when differentially expressed, affect the expression of related genes in the MAPK, autophagy, and apoptosis signaling pathways and thus the osteogenic function of BMSCs. In summary, the findings of this study indicate that MAP4K2 and CTSD exert significant influence on the proliferation, osteogenic differentiation, and mineralization processes of rat BMSCs cells. Furthermore, these proteins may contribute to the development of OP through their involvement in the regulation of autophagy and apoptosis. Conversely, our investigation did not reveal any discernible impact of SPI1 on OP-related phenotypes. Consequently, this research serves as a fundamental basis for further exploration of potential therapeutic targets for the treatment of OP.

Keywords Osteoporosis · Genetics · BMSCs · MAP4K2 · SPI1 · CTSD

Introduction

Osteoporosis is a systemic skeletal disorder that is characterized by diminished bone mass and deterioration of bone tissue microstructure, resulting in heightened bone

These authors contributed equally: Chao Sun, Wanxiong He, Leipeng Wang

These authors jointly supervised this work: Mingqi Sun, Feng Zheng, Baoxin Zhang

✉ Mingqi Sun
sunmingqi123456@163.com

✉ Feng Zheng
hydgk2011@163.com

✉ Baoxin Zhang
20150128@immu.edu.cn

Chao Sun
sunchao19870517@163.com

Wanxiong He
nyd2020120357@163.com

Leipeng Wang
2572816429@qq.com

[1] The Second Affiliated Hospital of Inner Mongolia Medical University, Hohhot, China

[2] Inner Mongolia Medical University, Hohhot, China

[3] Bayannur hospital, Bayannur, China

[4] Department of Hepatic Hydatidosis, Qinghai Provincial People's Hospital, Xining, Qinghai, China

[5] Tianjin Hospital, Tianjin University, Hexi District, Tianjin, China

fragility and susceptibility to fractures [1]. The incidence of fractures associated with OP tends to rise notably among women aged 55 and older, as well as men aged 65 and older [2]. Given the systemic nature of OP, the elevated risk of fractures affects virtually all skeletal sites [3]. Specifically, reduced hip bone mineral density (BMD) and spine BMD have been strongly linked to hip fractures and vertebral fractures, respectively, and have traditionally been regarded as the archetypal osteoporotic fractures [4]. Hip fractures are associated with reduced quality of life, a hip fracture is associated with a reduction in quality of life, an elevated risk of short-term mortality, and a considerable financial burden on healthcare systems [5]. Spinal fracture represents the most prevalent fracture associated with bone fragility, accounting for a considerable proportion of incidence, mortality, and other adverse health outcomes [6]. OP contributes to a large number of bone-related diseases and increases mortality and healthcare costs.

OP is a significant contributor to a multitude of bone-related ailments, leading to heightened mortality rates and increased healthcare expenditures. In order to sustain bone integrity, bones undergo continual remodeling processes throughout an individual's lifespan. This remodeling entails the meticulous regulation and harmonious equilibrium between osteoclasts and osteoblasts, which are responsible for maintaining bone mass and strength. Of particular importance are the osteocyte that differentiate from osteoblasts and are situated within mineralized bone, as they play a crucial role in the regulation of bone remodeling through various signaling pathways [7]. Disturbances in the balance between bone resorption and bone formation can lead to pathological abnormalities in BMD, a quantitative characteristic used as a surrogate phenotype for the diagnosis of OP [8]. The changes in BMD are influenced by a combination of both environmental and genetic factors. Studies focusing on genetics have indicated that the impact of genetic factors on BMD may vary across different skeletal sites; however, on the whole, ~50–85% of BMD alterations can be attributed to genetic factors [9]. Given the substantial occurrence of OP and the considerable heritability of associated skeletal characteristics, genetic investigations have the potential to elucidate pertinent biological mechanisms that may be therapeutically targeted for the management of this intricate and multifaceted ailment [10]. In most cases, genetic effects are determined by genetic variation in a large number of genes with small effect sizes, and in a few cases, a single mutation in a gene has a significant effect on bone mass or bone strength [10, 11]. Regardless of the magnitude of a gene's effect on disease, the identification of these genes has largely increased our understanding of the pathways that regulate bone homeostasis.

In our previous study, we identified a set of genes that potentially exhibit differential expression in OP. Among these genes, 10 hub genes were identified, namely TNF, RARRES2, FLNA, STXBP2, EGR2, MAP4K2, NFKBIA, JUNB, SPI1, and CTSD [12]. By searching relevant articles and combining the results of bioinformatics analysis, MAP4K2, SPI1, and CTSD were finally selected for further study. The objective of this study is to evaluate the effects of MAP4K2, SPI1, and CTSD on the osteogenic ability of BMSCs and to explore whether they may affect BMSCs through related mechanisms such as the MAPK signaling pathway, autophagy, and apoptosis. This will enable us to investigate the potential roles of MAP4K2, SPI1, and CTSD in OP.

Material and Methods

Extraction and Culture of BMSCs

Unless otherwise specified, all cells were cultured under standard conditions (37 °C and 5% CO_2) in DMEM complete medium (Wuhan Punosai, 164210) containing 10% fetal bovine serum(FBS) (Wuhan Punosai, PM150210). SD rats were deeply anaesthetised by intraperitoneal injection with 10% chloral hydrate solution and then immersed in 75% ethanol for 30 min. The epiphyses of femur and tibia were cut aseptically and immersed in phosphate buffered saline (PBS) (Nanjing Shengxing Biologicals, SN331) spiked with penicillin-streptomycin solution (double antibiotic) (Wuhan Pnosay, PB180120), and the epiphyseal cavities were rinsed with the culture solution (DMEM + 10% FBS + 1% double antibiotic) using a 5 ml syringe until the epiphyses turned white. After repeatedly blowing the cell suspension using a 1 ml pipette, the cell suspension was transferred to a culture flask and placed in a cell culture incubator at 37 °C with 5% CO_2.

When the cell confluence of BMSCs was 70–90%, the medium in the culture flasks was discarded, and sterile PBS (Nanjing Shengxing Biology, SN 331) was added and rinsed once. After adding 1 ml of 0.25% trypsin (Hyclone, SH30042.01, USA) for 30 s, double the volume of medium was added, and the cells in the wall of the culture flask were blown using a pipette, and the blowing was stopped when a large number of cells were detached in a floating state as observed by the microscope. The liquid from the culture flask was transferred to a sterilized 15 ml centrifuge tube and centrifuged at 1000 rpm for 5 min. The supernatant of the centrifuge tube was removed and fresh medium was added and blown well to resuspend the cells in the medium. 1 ml of medium was added to each well for incubation and used

for subsequent experiments. The passage number of BMSCs used in all subsequent experiments was between passage 3 and passage 5.

Flow Cytometry Analysis of BMSCs

After 2 passages, cells were examined by flow cytometry analysis. The cell suspension was taken, incubated with CD34 antibody (Abcam, UK, ab81289), centrifuged, cells washed, and then resuspended in PBS; Goat Anti-Rabbit (Alexa Fluor® 647) antibody was added, incubated, centrifuged, and cells were washed; and FITC-CD29 (Biolegend, USA, 102205) antibody was added. Incubation on ice protected from light, centrifugation. The cell suspension was incubated with FITC-CD90 (Biolegend, 206105, USA) and APC-CD45 (eBioscience, 17-0461-82, USA) antibodies and centrifuged on ice, protected from light. Cells were resuspended by adding PBS and immediately detected on a flow cytometer (BD, FACScalibur, USA).

Construction of Cellular Models of Alcoholic OP

The cell concentration was adjusted to 5×10^3 cells/well, and the cells were inoculated into 96-well plates and cultured in a cell culture incubator at 37 °C with 5% CO_2. After 1 day of cell culture, the medium was replaced with DMEM complete culture medium containing osteogenic induction solution (containing 10% FBS) and different concentrations of ethanol (Shanghai Sinopharm Group, 10009218) were added according to the subgroups, and the induction was continued for 1, 3, and 5 days, respectively. The specific groups were as follows: blank group (Control), 0.03 M alcohol group, 0.09 M alcohol group, 0.15 M alcohol group.

Cell Transfection

BMSCs were inoculated in 12-well plates at a concentration of 1×10^5/ml, and 1 ml of medium (without antibiotics) was added to each well and cultured for 12 h. Subsequently, we mixed the diluted MAP4K2 knockdown plasmid (Wuhan Miaoling Biologicals), negative control vector (Wuhan Miaoling Biologicals), SPI1 knockdown plasmid (Wuhan Miaoling Biologicals), negative control vector (Wuhan Miaoling Biologicals), CTSD overexpression plasmid (Wuhan Miaoling Biologicals), negative control vector (Wuhan Miaoling Biologicals) with Lipo8000™ transfection reagent (Shanghai Biyuntian, C0533) respectively. Miaoling Biologicals) were mixed with Lipo8000™ Transfection Reagent (Shanghai Biyuntian, C0533), and left to stand for 1 min at room temperature, then added to the cell culture wells of the corresponding groups, and shook well. The cells were placed in a 37 °C, 5% CO_2 incubator for 24 h, and then the cells were changed to continue the culture. When the cell confluence was 70–90%, the cells were digested and inoculated into cell culture flasks and 12-well plates. After 13 days of transfection, the expression of MAP4K2, SPI1, and CTSD was determined by qRT-PCR, and the transfected cells were passaged and used for downstream analysis.

Osteogenic Induction and Grouping

Osteogenic media: Dexamethasone (MCE, HY-14648) was dissolved in ethanol (Shanghai Sinopharm Group, 10009218) at a concentration of 1 mM. Ascorbic acid (Beijing Sololebao, A8100) was dissolved using PBS (Nanjing Shengxing Biology, SN 331) at a concentration of 10 mM. β-glycerophosphate (Beijing, G8100) was dissolved in PBS at a concentration of 1 M. Medium without serum was added successively, and the final concentration of each component was 0.1 μM dexamethasone, 0.2 mM ascorbic acid, and 10 mM β-glycerophosphate sodium. Use 0.22 μM filter and save for 4 °C.

The cell suspension (undifferentiated BMSCs) was filled with the cover glass and the counting plate, and left for 2–3 min. Calculate the cells in four large squares (composed of small squares of 44) for the total cell amount.The cell concentration was adjusted to 5×10^3 cells/well, and the cells were inoculated into 96-well plates and placed in a cell culture incubator at 37 °C with 5% CO_2. After 1 day of cell culture, the cells were treated according to the following groupings: (i) model group (AOP): induction by modeling optimal concentration of alcohol (0.15 M); (ii) knockdown control + optimal alcohol group (KO-NC): induction by modeling optimal concentration of alcohol (0.15 M), and simultaneous transfection of knockdown control plasmid; (iii) optimal alcohol + MAP4K2 knockdown group (KO-MAP4K2): induction by modeling optimal concentration of alcohol (0.15 M); (iv) KO-MAP4K2 knockdown group (KO-MAP4K2): induction by modeling optimal concentration of alcohol (0.15 M), and transfection of knockdown control plasmid. (v) Optimal alcohol + overexpression control (OE-NC): induced by the optimal concentration of alcohol (0.15 M) and transfected with the control plasmid; (vi) Optimal alcohol + CTSD overexpression plasmid. Optimal alcohol + CTSD overexpression group (OE-CTSD): induced by modeling optimal concentration of alcohol (0.15 M) and transfected with CTSD overexpression plasmid. The medium was replaced with DMEM complete culture medium (containing 10% FBS) for osteogenic induction.

Cell Viability Assay

After the corresponding time of osteogenic induction, different groups of cells were collected for CCK-8 assay. CCK-8 solution (Shanghai Biyuntian, C0037) with 10% of culture medium was added to each well, and continued to be placed in the cell culture incubator at 37 °C and 5% CO_2 for 2–3 h. 100 µl of each well was aspirated into a 96-well plate, and the OD value was determined. The absorbance value (OD value) of each well was measured at 450 nm on an enzyme labeling instrument, and finally, the results were counted, and the relative cell viability (%) was calculated using the formula. Relative cell viability (%) = OD450'/avg(OD450C') × 100%, OD450': absorbance value of the test group minus the zero-adjusted group, avg (OD450C'): average absorbance value of the corrected control group. Zero adjusted group: refers to the control group where cell viability is measured under baseline conditions without any treatment.

ALP Activity and ALP Staining Assay

After 7 d of continuous osteogenic induction, different groups of cells were collected for ALP activity (content) assay and ALP staining. The total protein concentration was determined using the BCA Protein Concentration Assay Kit (Beyotime, Shanghai, P0010) according to the manufacturer's instructions, and using the ALP activity assay kit (micro enzyme-linked immunosorbent assay) (Nanjing Jiancheng, A059-2) to detect and analyze ALP protein activity in cell supernatant. The unit of cell viability is Kings/gprot. Each gram of tissue protein reacts with the matrix at 37 °C for 15 min to produce 1 mg of phenol, which is means 1 Kings/gprot. G is the weight gram, and prot refers to protein. For ALP staining, the original medium was first removed and rinsed with PBS for 3 times. Add 4% paraformaldehyde solution for fixation for 20 min, rinse with PBS 3 times for 5 min each. Prepare 5-bromo-4-chloro-3-indolyl phosphate(BCIP) /nitro blue tetrazolium (NBT) staining working solution (Shanghai Biyuntian, C3206) according to the instruction and add it to the well plate, incubate at room temperature and away from light for 18 h, and wash with distilled water twice. The stained cells were observed and recorded under an inverted microscope. BCIP and NBT are chromogenic substrates used in histochemical staining to visualize alkaline phosphatase activity. The reaction produces a blue-purple precipitate, allowing for the localization of the enzyme in tissue samples.

Alizarin Red Staining

After 21 d of continuous induction of osteogenesis in different groups of rat BMSCs cells, the original medium was removed, 95% ethanol was added to fix the cells for 30–60 min, and the cells were rinsed with PBS for 3 times, then 1% Alizarin Red (Beijing, G1452) solution was added, and staining was carried out for 30 min at room temperature. At the end of the staining process, the cells were rinsed with PBS for several times until there was no obvious color and suspensions in the rinsing solution, and the stained cells were observed through an inverted microscope.

RNA Isolation and qRT-PCR

The culture medium was replaced with DMEM complete culture medium (containing 10% FBS) containing osteogenic induction solution, i.e., after 21 d of continuous osteogenic induction, the cells were collected. Total RNA samples were extracted from BMSCs using Trizol reagent (Takara, Japan, 9108) and RNAeasy™ Animal RNA Extraction Kit (Shanghai Biyuntian, R0024). The OD values of the samples were determined using a microspectrophotometer and the absorption values at 260 nm and 280 nm were observed to determine the quality of the RNA. When A260/A280 is between 1.8 and 2.0, the RNA quality is better, and the better quality RNA can be used directly in the next experiment. Total RNA was reverse transcribed into cDNA using a cDNA synthesis kit (Shanghai Biyuntian, D7168S). RT-PCR was performed using AceQ qPCR SYBR Green Master Mix (Low ROX Premixed) (Nanjing Vazyme, Q131-02) under the following reaction conditions: Pre-denaturation 95 °C for 5 min, cycle 1 time; denaturation 95 °C for 10 s, annealing extension 60 °C for 35 s, cycle 40 times. Melting curve 95 °C 15 s, 60 °C 60 s, 95 °C 15 s, continuous detection signal. At the end of the reaction, the PCR product specificity was confirmed by melting curve analysis with or without spurious bands and primer dimers. The Ct value of each sample was obtained, and the relative expression of mRNA of each sample was analyzed by the $2^{-\Delta\Delta Ct}$ method. the PCR primers are shown in Table 1. The primers used in the study were designed using Primer3 software.

Statistical Analysis

The data obtained from the experiments were expressed as mean ± standard deviation (Mean ± S.D.), and all data were processed and statistically analyzed using GraphPad Prism 6. Comparisons between the sample means of two groups were made using the t-test, and comparisons between the sample means of multiple groups were made using the analysis of variance (ANOVA) test, with $P < 0.05$ indicating that the difference was statistically significant.

Table 1 Primers of MAP4K2, SPI1, CTSD, p38, TRAF6, LC3, p62, Bcl-2, Bax, Caspase3 and GAPDH

Gene	Sense and antisense (5′-3′)	
Rat MAP4K2	F	ACCGCTTGTGGATATGTATGG
	R	TAGGCAATCTGCCGTTCTTC
Rat SPI1	F	ATTGATCCCCACCGAAGCAG
	R	AACCCTTCCATTTTGCACGC
Rat CTSD	F	GGCAACCTGGAGGAGAACTAA
	R	TTGGCAAAGCCGACCCTAT
Rat p38	F	CAGCTAATGTTCTGCACCGT
	R	ACGCGTGGCTACATACTCTG
Rat TRAF6	F	AGGGTACAATACGCCTCACG
	R	GCTACACGCCTGCATCAGTA
Rat LC3	F	CATGCCGTCCGAGAAGACCT
	R	GATGAGCCGGACATCTTCCACT
Rat p62	F	GCCCTGTACCCACATCTCC
	R	CCATGGACAGCATCTGAGAG
Rat Bcl2	F	TATATGGCCCCAGCATGCGA
	R	GGGCAGGTTTGTCGACCTCA
Rat Bax	F	ATCCAAGACCAGGGTGGCTG
	R	CACAGTCCAAGGCAGTGGGA
Rat caspase-3	F	ACGGTACGCGAAGAAA-AGTGAC
	R	TCCTGACTTCGTATTTCAGGGC
Rat GAPDH	F	TGAAGGTCGGAGT CAACGG
	R	CCTGGA AGATGGTGATGGG

Results

Culture, Identification, and Alcoholic OP Cell Model Construction of BMSCs in SD Rats

The normal SD rat BMSCs were observed to be predominantly stretched pike or polygonal in shape, with a few irregularly rounded, mononuclear, monolayer-adherent growths displaying an irregular arrangement. At the 2-day mark of the primary culture period, the cells demonstrated enhanced adhesion to the wall, accompanied by a gradual proliferation over time. However, an increase in heterocytes (rounded) was observed (Fig. 1a). As the cell passaging multiplicity increased, the proportion of heterocytes decreased, and the cells were prepared for subsequent experiments at the third generation (Fig. 1b). The results of the flow cytometry analysis of the rat BMSCs are presented in Fig. 1c. The BMSCs were positive for CD90 and CD29 and negative for CD45 and CD34. The results of the flow cytometry analysis demonstrated that ~93.4% of the total cells were CD90-positive, ~94.2% were CD29-negative, ~94.2% were CD45-negative, and ~93.7% were CD34-negative.

Following a 21-day osteogenic induction period, the cellular alizarin red staining results of rat BMSCs in each experimental group are presented in Fig. 1d. Upon examination under an inverted microscope, it was evident that red mineralized nodules (indicated by black arrows) were present following cellular alizarin red staining, with notable cellular mineralized nodules observed in the Control group. In comparison to the control group, the mineralization nodules of the rat BMSCs in the alcohol groups (0.03 M, 0.09 M, and 0.15 M) exhibited a gradual decline with the increase in alcohol concentration. Following a 7-day osteogenic induction period, the results of ALP staining of rat BMSC cells in each group are presented in Fig. 1e. Under the inverted microscope, it can be observed that the ALP-positive cells were stained with a blue-purple color. In comparison to the Control group, the ALP staining of rat BMSCs cells in the 0.03 M, 0.09 M, and 0.15 M alcohol groups exhibited a gradual decrease in intensity with the increase of alcohol concentration. This indicated a corresponding reduction in positive expression. Figure 1f illustrates the proliferation levels of rat BMSCs cells in each group after 1, 3, and 5 days of osteogenic induction. The CCK-8 results demonstrated that there was no statistically significant difference in the viability of rat BMSCs cells in each group after 1 d of osteogenic induction. The viability levels of the rat BMSCs in the 0.09 M and 0.15 M alcohol groups were significantly reduced in comparison to the Control group after 3 days of osteogenic induction. Similarly, after 5 days of osteogenic induction, the viability levels of the rat BMSCs in the 0.03 M, 0.09 M and 0.15 M alcohol groups were significantly reduced in comparison to the Control group.

Based on the effects of different alcohol concentrations on cell viability as well as osteogenic capacity, we chose 0.15 M as the concentration used for subsequent model construction.

Successful Establishment of Differential Expression System of MAP4K2, SPI1, and CTSD in BMSCs

The results of comparison of the mRNA expression levels of MAP4K2, SPI1, and CTSD in the cells of each group after transfection of rat BMSCs cells are shown in Fig. 2. qRT-PCR experiments showed that, after transfection of rat BMSCs cells, the mRNA expression levels of MAP4K2 and SPI1 in the cells of KO-MAP4K2 group and KO-SPI1 group were significantly reduced, compared with KO-NC group; and the mRNA expression levels of CTSD in the cells of OE-CTSD group were significantly increased, compared with those of OE-NC group. The above results indicate that the differential expression system of MAP4K2, SPI1 and CTSD in rat BMSCs cells has been established, and the subsequent experiments will be carried out on this basis.

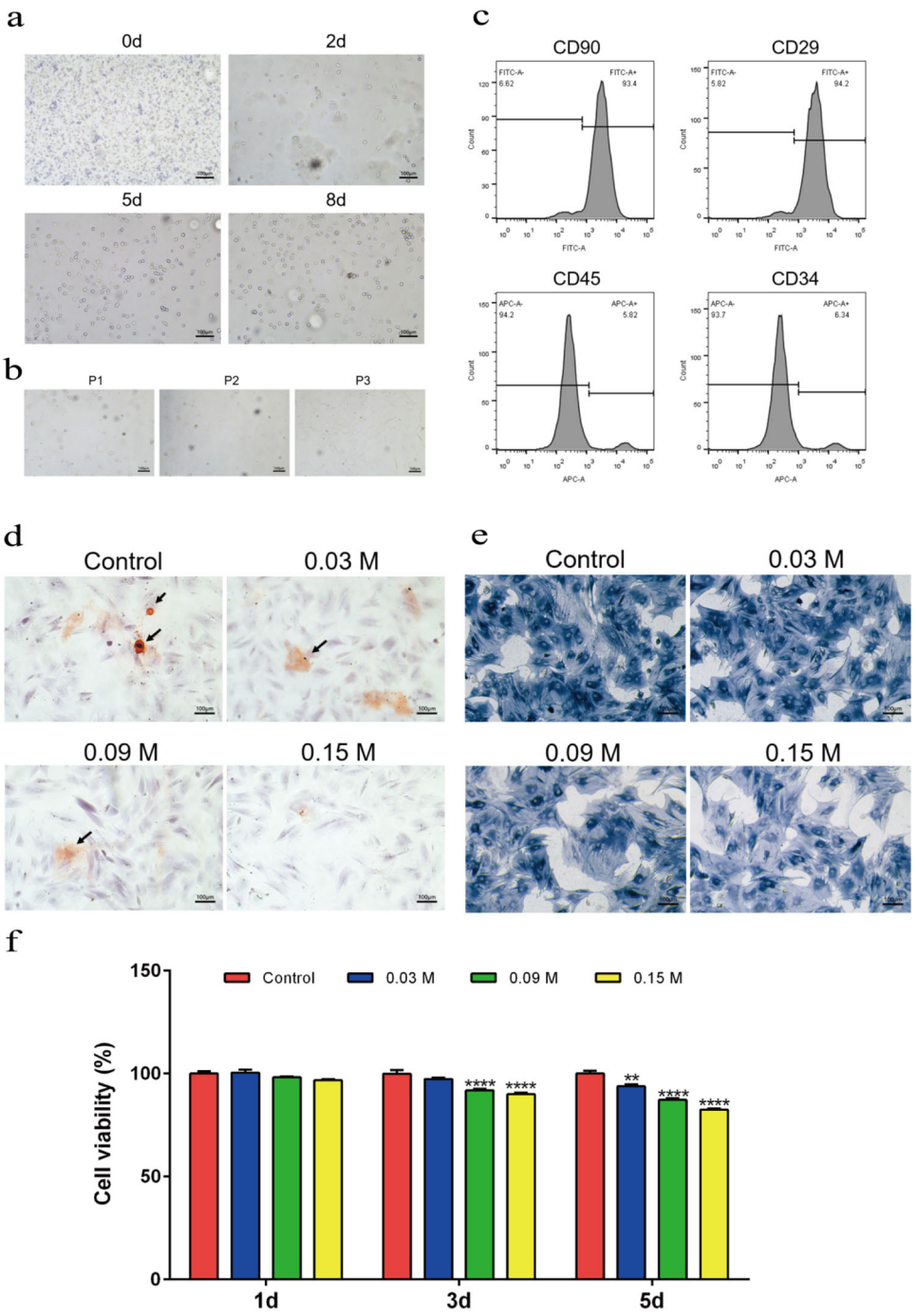

Fig. 1 **a** Morphological observation under the inverted microscope of BMSCs primary culture (100×) (**b**) Morphological observation under the inverted microscope of BMSCs progeny culture (100×) (**c**) Results of flow identification of primary rat BMSCs (**d**) Comparison of the results of alizarin staining in the cells of BMSCs of rats of all groups after 21 d of osteogenesis (100×) (**e**) Comparison of ALP staining results of rat BMSCs cells in each group after 7 d of osteogenic induction (100×) (**f**) Comparison of cell viability of rat BMSCs cells in each group after 1, 3, and 5 d of osteogenic induction (** $P < 0.01$, **** $P < 0.0001$ vs. Control), and P values were calculated using the ANOVA test

MAP4K2 and CTSD Affect the Viability of BMSCs

The results of the comparison of cell viability in each group after 1, 3, 5, and 7 days of osteogenic induction of rat BMSCs cells are shown in Fig. 3. The results of CCK-8 assay showed that, compared with the AOP group, there was no significant difference between the cells of each group after 1 and 3 days of osteogenic induction; the cell viability of the KO-MAP4K2 group and the OE-CTSD group were both significantly elevated after 5 and 7 days of osteogenic induction.

KO-MAP4K2 and OE-CTSD Promote Osteogenic Differentiation of BMSCs

The results of comparison of ALP activity of cells in each group after 7 days of osteogenic induction of rat BMSCs cells are shown in Fig. 4. The results of ALP activity assay

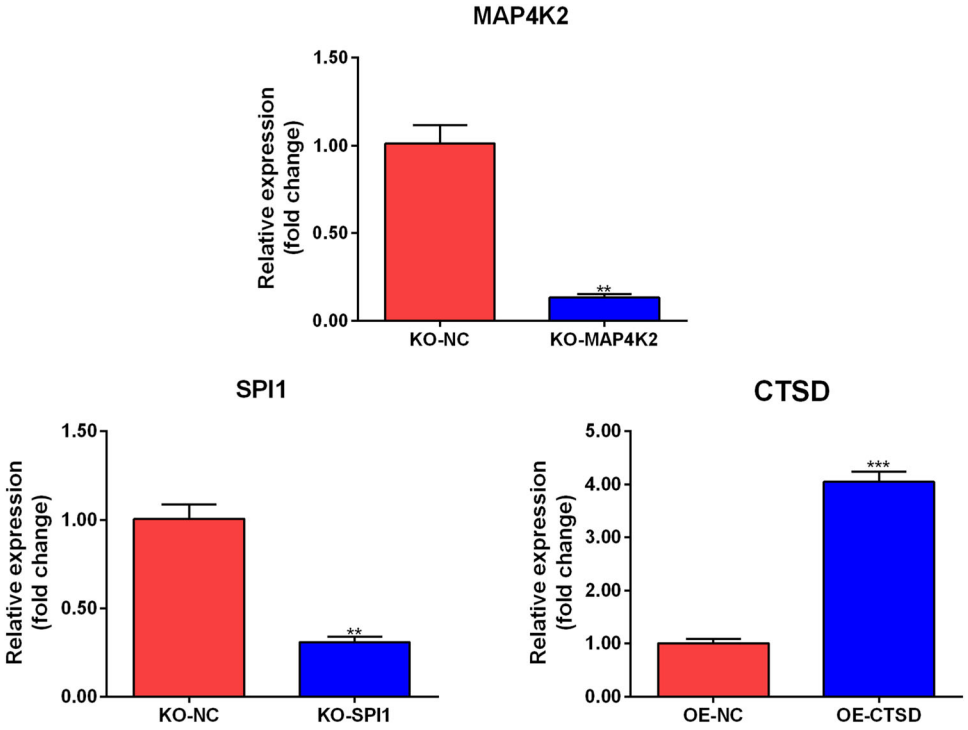

Fig. 2 Comparison of mRNA expression levels of MAP4K2, SPI1, and CTSD after transfection of rat BMSCs, P values were calculated using a two-sided unpaired Student t test (** $P < 0.01$, *** $P < 0.001$ vs. OE-NC or KO-NC, $n = 3$)

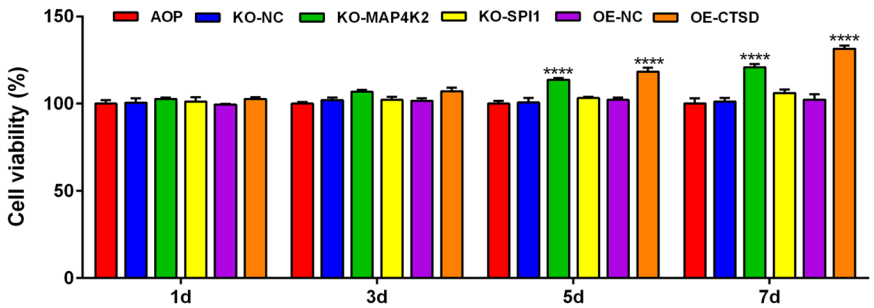

Fig. 3 Comparison of cell activity after 1, 3, 5, and 7 days of osteogenic induction of rat BMSCs in each group, P-values were calculated using the ANOVA test (**** $P < 0.0001$ vs. AOP, $n = 3$)

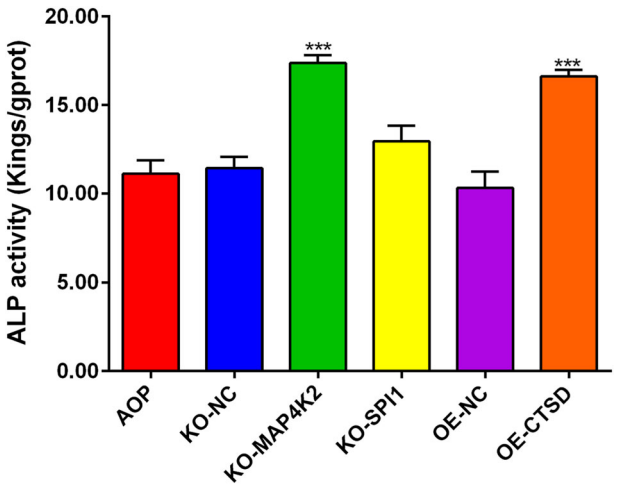

Fig. 4 Comparison of ALP activity after 7 days of osteogenic induction of rat BMSCs in each group, P-values were calculated using the ANOVA test (*** $P < 0.001$ vs. AOP, $n = 3$)

showed that ALP activity was significantly elevated in the cells of KO-MAP4K2 and OE-CTSD groups, compared with that of AOP group.

The results of ALP staining of cells in each group after 7 days of osteogenic induction of rat BMSCs are shown in Fig. 5. Under the inverted microscope, it can be observed that the ALP-positive cells showed purple. Among them, the ALP staining of cells in AOP, KO-NC, KO-SPI1 and OE-NC groups was relatively light, while the ALP staining of cells in KO-MAP4K2 and OE-CTSD groups was relatively dark.

MAP4K2 and CTSD Affect the Ability of BMSCs to Calcify

After 21 days of osteogenic induction of rat BMSCs, the results of alizarin red staining of cells in each group are shown in Fig. 6. Under the inverted microscope, it can be

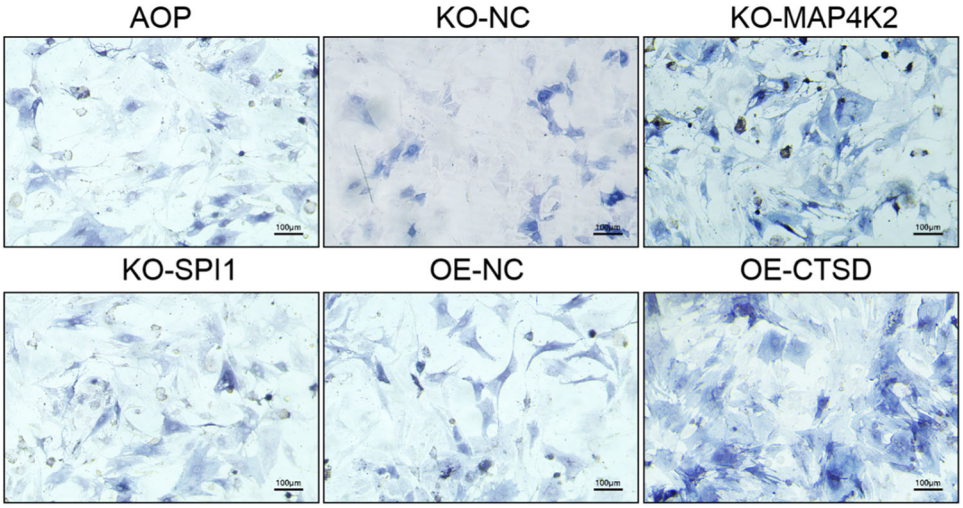

Fig. 5 Comparison of ALP staining results after 7 days of osteogenic induction of rat BMSCs in each group (100×, $n = 3$)

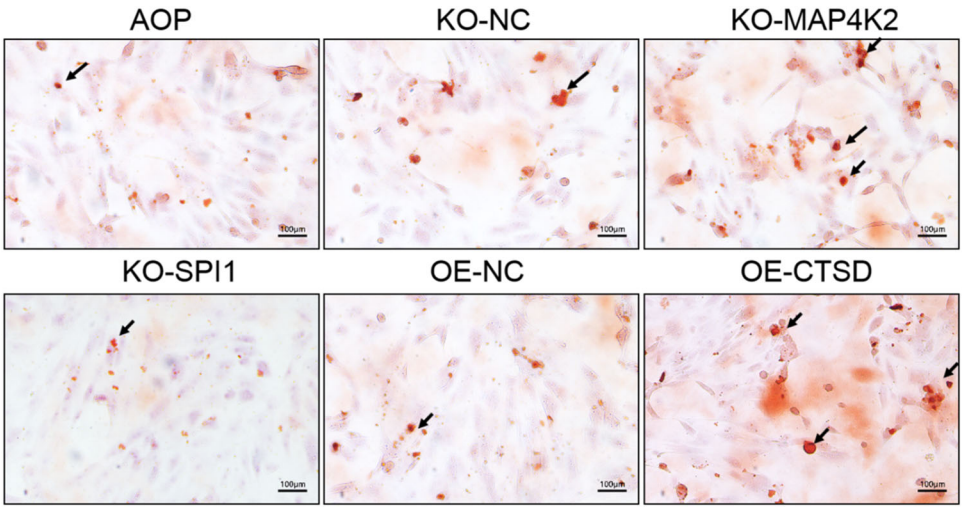

Fig. 6 Comparison of alizarin red staining results after 21 days of osteogenic induction of rat BMSCs in each group (100×, n = 3)

observed that some of the cells were visible as red mineralized nodules after alizarin red staining (black arrowheads). Among them, the number of calcium nodules in the cells of AOP group, KO-NC group, KO-SPI1 group, and OE-NC group was relatively small, while the number of calcium nodules in the cells of KO-MAP4K2 group and OE-CTSD group increased.

Expression of Related Molecules in Rat BMSCs

After 21 days of osteogenic induction in rat BMSCs, the results of comparison of mRNA expression levels of MAP4K2, SPI1, CTSD, p38, TRAF6, LC3, p62, Bcl-2, Bax, and Caspase3 in the cells of each group are shown in Fig. 7. The results of the qRT-PCR experiments showed that, in comparison with the AOP group, mRNA expression levels of MAP4K2, Bax, and Caspase3 were significantly reduced in cells of the KO -MAP4K2 group cells, the mRNA expression levels of MAP4K2, Bax, and Caspase3 were all significantly reduced, and the mRNA expression levels of p38, LC3, p62, and Bcl-2 were all significantly increased; the mRNA expression levels of SPI1 were significantly reduced in the cells of the KO-SPI1 group, while no significant differences were observed in the mRNA expression levels of any other genes. There was no significant difference in the mRNA expression levels of other genes; the mRNA expression levels of Bax and Caspase3 in the OE-CTSD group were significantly reduced, and the mRNA expression levels of CTSD, LC3, p62, and Bcl-2 were significantly increased.

Discussion

As OP is a serious health problem, a large amount of research has focused on elucidating the etiology of the disease as well as identifying new therapeutic targets for the treatment of patients with OP. These studies have shown that substantial changes in bone mass and strength are often

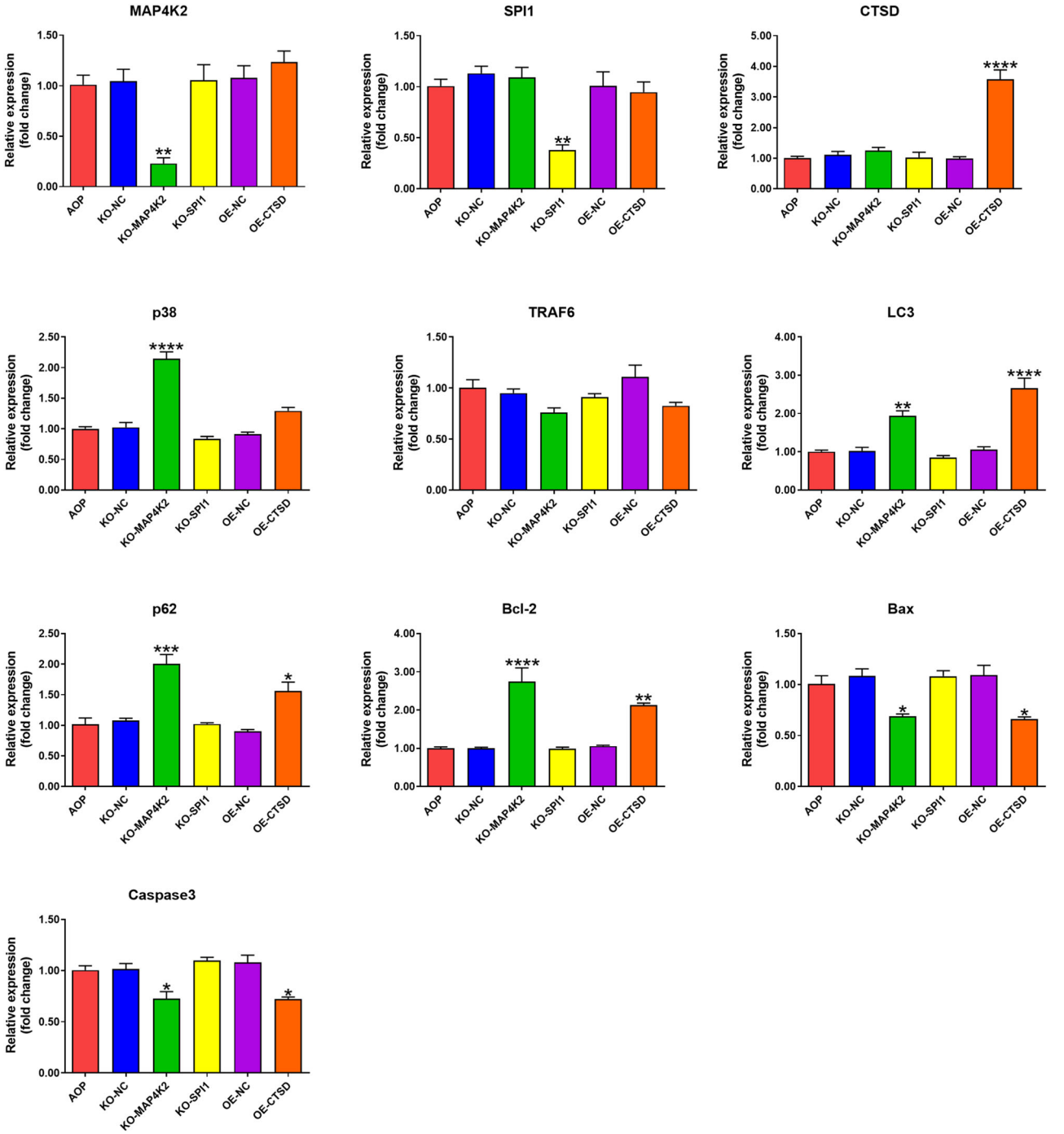

Fig. 7 Comparison of mRNA expression levels of 12 genes after 21 days of osteogenic induction of rat BMSCs in each group, P-values were calculated using the ANOVA test (*$P < 0.05$, **$P < 0.01$, ***$P < 0.001$, ****$P < 0.0001$ vs. AOP, $n = 3$)

influenced by genetic variation in genes encoding important regulators of bone homeostasis [13]. Over the years, studies of the genetic causes of OP and of several rare single-gene disorders with abnormally high or low bone mass and strength have greatly increased the understanding of the regulatory pathways important for bone resorption and formation [14].

In our previous study, we used bioinformatics to identify MAP4K2, SPI 1, and CTSD as OP Hub genes [12]. These genes have been the subject of several studies, Ma et al. [15] found that MAP4K2 protein expression was associated with the degree of differentiation in colorectal cancer, in addition, Zhang et al. [16] showed increased expression of MAP4K2 upstream of JNK in aging osteoblasts.Spi-1, a

member of the Ets family of transcription factors, is predominantly found in myeloid cells (granulocytes, monocytes, and macrophages) and in B cells expression [17], YANG C et al. [18] found in their study that TET2 interacts with SPI1 to regulate the expression of genes critical for osteoclast differentiation.CTSD is an aspartic acid-type protease universally expressed in all cells of the human body and is essential for neuronal cellular homeostasis, and it has been shown that CTSD-mediated protein hydrolysis plays a unique role in the pathogenesis of human neurodegenerative diseases [19], and it has also been reported that CTSD plays a role in regulating the severity of acute pancreatitis [20], and Deng et al. [21] established a model of postmenopausal OP in rats by bilateral oophorectomy, and found that the CTSD of blood monocytes in the OVX group was lower than that in the control group. However, no further studies have been conducted on the possible roles of MAP4K2, SPI 1, and CTSD in OP.

Previous studies have shown that stem cells play an important role in the development of OP, and the development of OP was inhibited in animal models after promoting osteogenic differentiation of BMSCs [22, 23], therefore, we used rat BMSCs as a cellular model of OP, and established a system of differential expression of MAP4K2, SPI1, and CTSD in rat BMSCs cells by transfection. In order to determine the effects of MAP4K2, SPI1, and CTSD on the activity of BMSCs, CCK-8 experiments were subsequently carried out in different groups, and the results showed that the cellular viability was significantly increased in the KO-MAP4K2 group and the OE-CTSD group, while there was no significant difference in the KO-SPI1 group. The increase of the viability of BMSCs in the KO-MAP4K2 group and the OE-CTSD group implies that knockdown of MAP4K2 and overexpression of CTSD are likely to be beneficial for OP patients.

In order to further verify the effects of MAP4K2, SPI1, and CTSD on rat BMSCs cells, we performed ALP activity assay and staining, ALP, as an essential enzyme, appears in the early stages of osteogenic differentiation [24], and increased ALP expression in bone represents increased osteogenic differentiation [25], 7 days after osteogenic induction in rat BMSCs cells, ALP activity was significantly elevated in the cells of both MAP4K2 and OE-CTSD groups. Subsequently, the results of ALP staining of cells in each group were consistent with the results of ALP activity assay The ALP staining of cells in the KO-SPI1 group was relatively lighter, while the ALP staining of cells in the KO-MAP4K2 group and the OE-CTSD group was relatively darker. The results of alizarin red staining of the cells in each group were also consistent with the ALP activity assay. The number of calcium nodules in the cells of the KO-SPI1 group was relatively low, whereas the number of calcium nodules in the cells of the KO-MAP4K2 group and the OE-CTSD group was increased. OP is characterized by a decrease in bone strength, leading to an increased risk of fracture [26], bone remodeling is a process that affects bone strength, through which old bone is resorbed and then new bone is formed [27, 28], reduced bone resorption and increased bone formation each produce a positive bone balance, is for OP treatment is an effective regimen [29], MAP4K2, CTSD in rat The positive role of MAP4K2, CTSD in osteogenesis and mineralization of BMSCs cells suggests that they may play an important role in OP development.

In order to verify whether there is a difference in the expression of MAP4K2, SPI1, CTSD and to preliminarily investigate whether the differential expression of MAP4K2, SPI1, CTSD affects the expression of related genes in MAPK, autophagy and apoptosis signaling pathways and thus affects the osteogenic function of BMSCs, we detected the expression levels of the MAPK signaling pathway-related molecules as p38 in the cells of each group, TRAF6, autophagy-related molecules LC3 and p62, and apoptosis-related molecules Bcl-2, Bax, and Caspase3 in each group [30–33]. The results of qRT-PCR showed that the expression level of MAP4K2 was significantly reduced in the KO-MAP4K2 group, and the expression of genes related to MAPK signaling pathway (p38), autophagy (LC3, p62) and apoptosis signaling pathway (Bcl-2, Bax, Caspase3) also differed, and the increased expression of p38, LC3, p62 and Bcl-2 and the significant reduction of Bax and Caspase3 suggested that MAP4K2 might be involved in the disease development of OP through shadowing the MAPK signaling pathway, autophagy, and apoptosis. The increase in p38, LC3, p62, and Bcl-2 and the significant decrease in Bax and Caspase3 suggest that MAP4K2 may be involved in the disease development of OP by shadowing the MAPK signaling pathway, autophagy, and apoptosis. The mRNA expression level of SPI1 was significantly reduced in the KO-SPI1 group, and there were no significant differences in the mRNA expression levels of other genes. CTSD expression levels were significantly increased in the OE-CTSD group, and the expression of genes related to autophagy (LC3, p62), apoptosis signaling pathway (Bcl-2, Bax, Caspase3) these pathways were also varied. The increase in LC3, p62, and Bcl-2 and the significant decrease in Bax and Caspase3 suggest that CTSD may be involved in the disease development of OP by affecting autophagy and apoptosis.

In a previous qRT-PCR experiment, it was found that the mRNA expression levels of MAP4K2 and SPI1 in the serum of the OP group were both significantly higher, and the mRNA expression level of CTSD was significantly lower than that of the control group [12]. The experimental results in this article showed that knockdown of MAP4K2 and overexpression of CTSD were consistent with the

expected results suggested in previous studies and positively affected BMSCs osteogenesis, further validating that MAP4K2 and CTSD may be new therapeutic targets for OP prevention, diagnosis, and treatment and that SIP1 was shown in our experiments to be altered without affecting the cell viability, osteogenic differentiation and mineralized nodule formation of BMSCs.

In patients with OP, despite advances in fracture risk assessment and the development of a range of medications to reduce fractures [34], treatment rates in high-risk individuals remain low [35]. Identifying the genetic factors that regulate BMD has proved challenging over the last few decades. The identification of causative genes has increased the understanding of the regulation of BMD, further adding important signaling pathways and new therapeutic targets. The effects of MAP4K2 and CTSD on osteoporotic (OP) cell models have been preliminarily validated by our research team. These genes have potential applications in osteoporosis diagnosis and treatment.

Conclusion

The experimental results showed that MAP4K2 and CTSD affected the cell activity, osteogenic differentiation and calcification ability of rat BMSCs. SPI1, although differentially expressed in the OP and control groups, was not involved in the OP-related phenotypes. The effects of differential expression of MAP4K2 and CTSD on rat BMSCs have only been preliminarily explored. Thus far, the question of whether these genes have similar roles in human BMSCs remains unanswered. Furthermore, the potential molecular mechanisms by which MAP4K2 and CTSD exert these roles have yet to be fully elucidated. Further validation of the role of these genes in human OP cell models and in animal OP models is needed in the future, and their significance in the development and progression of osteoporosis can also be explored from the perspectives of proteomics and protein modifiers, and epigenetic influences.

Author Contributions Baoxin Zhang, Feng Zheng, and Mingqi Sun coordinated the study. Chao Sun, Wanxiong He, and Leipeng Wang analyzed the data and wrote the main manuscript text. Ting Hao, Xiaolong Yang, Wei Feng, Yonggang Wu, Chenyang Meng, Zhi Wang, and Xiaofeng Chen contributed reagents/materials and all biochemical and molecular results. All authors reviewed the manuscript.

Funding This work was supported by Inner Mongolia Science and Technology Department Science and Technology Plan Project (2020GG0195 and 2021GG0174), Inner Mongolia Autonomous Region Natural Science Foundation Project (2019MS008158 and 2023LHMS08031), Inner Mongolia Medical University Science and Technology Million Project (Joint) (YKD2018KJBW(LH)002), Mongolia Medical University Youth Leading Innovation "Bone to Muscle" Lecture Group (QNLC-20200030), Inner Mongolian Autonomous Region Higher Education Science Research Project (NJZZ22665), Inner Mongolia Autonomous Region's discipline construction project, distinctly marked as "funds to support the reform and development of local colleges and universities (discipline construction), The "Zhiyuan" Talent Program of Inner Mongolia Medical University (Z.Y. 20242146), "Inner Mongolia Autonomous Region Specialist Regional Medical Centre" Bayannur City Hospital Orthopaedic Department. Regional Science Foundation Project of National Natural Science Foundation of China (82460985), 2022 Qinghai Province "Kunlun Talents·High end Innovation and Entrepreneurship Talents" Project.

Compliance with Ethical Standards

Conflict of Interest The authors declare no competing interests.

Ethical Approval 1. All methods involving humans and animals were performed in accordance with the relevant guidelines and regulations. 2. All methods involving humans and animals were approved by the Second Affiliated Hospital of Inner Mongolia Medical University (ethics review number: YKD202002055). 3. All animal experiments were performed in accordance with ARRIVE guidelines.

Publisher's note Springer Nature remains neutral with regard to jurisdictional claims in published maps and institutional affiliations.

Open Access This article is licensed under a Creative Commons Attribution-NonCommercial-NoDerivatives 4.0 International License, which permits any non-commercial use, sharing, distribution and reproduction in any medium or format, as long as you give appropriate credit to the original author(s) and the source, provide a link to the Creative Commons licence, and indicate if you modified the licensed material. You do not have permission under this licence to share adapted material derived from this article or parts of it. The images or other third party material in this article are included in the article's Creative Commons licence, unless indicated otherwise in a credit line to the material. If material is not included in the article's Creative Commons licence and your intended use is not permitted by statutory regulation or exceeds the permitted use, you will need to obtain permission directly from the copyright holder. To view a copy of this licence, visit http://creativecommons.org/licenses/by-nc-nd/4.0/.

References

1. Foessl, I., Dimai, H. P., & Obermayer-Pietsch, B. (2023). Long-term and sequential treatment for osteoporosis. *Nature Reviews Endocrinology*, *19*, 520–533. https://doi.org/10.1038/s41574-023-00866-9.
2. Compston, J. E., McClung, M. R., & Leslie, W. D. (2019). Osteoporosis. *Lancet*, *393*, 364–376. https://doi.org/10.1016/S0140-6736(18)32112-3.
3. Stone, K. L., Seeley, D. G., Lui, L. Y., Cauley, J. A., Ensrud, K., Browner, W. S., Nevitt, M. C., Cummings, S. R., & Osteoporotic Fractures Research, G. (2003). BMD at multiple sites and risk of fracture of multiple types: Long-term results from the Study of Osteoporotic Fractures. *Journal of Bone Mineral Research*, *18*, 1947–1954. https://doi.org/10.1359/jbmr.2003.18.11.1947.
4. Marshall, D., Johnell, O., & Wedel, H. (1996). Meta-analysis of how well measures of bone mineral density predict occurrence of osteoporotic fractures. *The BMJ*, *312*, 1254–1259. https://doi.org/10.1136/bmj.312.7041.1254.
5. Oden, A., McCloskey, E. V., Johansson, H., & Kanis, J. A. (2013). Assessing the impact of osteoporosis on the burden of hip

fractures. *Calcified Tissue International*, *92*, 42–49. https://doi.org/10.1007/s00223-012-9666-6.
6. Schousboe, J. T. (2016). Epidemiology of vertebral fractures. *Journal of Clinical Densitometry*, *19*, 8–22. https://doi.org/10.1016/j.jocd.2015.08.004.
7. Hadjidakis, D. J., & Androulakis, I. I. (2006). Bone remodeling. *Annals of the New York Academy Sciences*, *1092*, 385–396. https://doi.org/10.1196/annals.1365.035.
8. Matsumoto, T., Sone, T., Soen, S., Tanaka, S., Yamashita, A., & Inoue, T. (2022). Abaloparatide increases lumbar spine and hip BMD in Japanese patients with osteoporosis: The phase 3 ACTIVE-J study. *The Journal of Clinical Endocrinology Metabolism*, *107*, e4222–e4231. https://doi.org/10.1210/clinem/dgac486.
9. Boudin, E., Fijalkowski, I., Hendrickx, G., & Van Hul, W. (2016). Genetic control of bone mass. *Molecular and Cellular Endocrinology*, *432*, 3–13. https://doi.org/10.1016/j.mce.2015.12.021.
10. Fijalkowski, I., Boudin, E., Mortier, G., & Van Hul, W. (2014). Sclerosing bone dysplasias: Leads toward novel osteoporosis treatments. *Current Osteoporosis Reports*, *12*, 243–251. https://doi.org/10.1007/s11914-014-0220-5.
11. Hendrickx, G., Boudin, E., & Van Hul, W. (2015). A look behind the scenes: The risk and pathogenesis of primary osteoporosis. *Nature Reviews Rheumatology*, *11*, 462–474. https://doi.org/10.1038/nrrheum.2015.48.
12. Wang, X., Pei, Z., Hao, T., Ariben, J., Li, S., He, W., Kong, X., Chang, J., Zhao, Z., & Zhang, B. (2022). Prognostic analysis and validation of diagnostic marker genes in patients with osteoporosis. *Frontiers in Immunology*, *13*, 987937. https://doi.org/10.3389/fimmu.2022.987937.
13. Raisz, L. G. (2005). Pathogenesis of osteoporosis: Concepts, conflicts, and prospects. *Journal of Clinical Investigation*, *115*, 3318–3325. https://doi.org/10.1172/JCI27071.
14. Boudin, E., & Van Hul, W. (2017). Mechanisms in endocrinology: Genetics of human bone formation. *European Journal of Endocrinology*, *177*, R69–R83. https://doi.org/10.1530/EJE-16-0990.
15. Ma, Q. Z., Yang, Y. W., Ma, Y. L., Liao, S. P., Zheng, Y. J., Zhang, S., Cao, Y. Y., Zhang, J., & Wang, Y. F. (2019). Correlation of K-ras gene mutations with the protein expressions of TAK1 and MAP4K2 in colorectal cancer. *Sichuan Da Xue Xue Bao Yi Xue Ban*, *50*, 61–65.
16. Zhang, X., Zhao, G., Zhang, Y., Wang, J., Wang, Y., Cheng, L., Sun, M., & Rui, Y. (2018). Activation of JNK signaling in osteoblasts is inversely correlated with collagen synthesis in age-related osteoporosis. *Biochemical and Biophysical Research Communications*, *504*, 771–776. https://doi.org/10.1016/j.bbrc.2018.08.094.
17. Chen, H., Ray-Gallet, D., Zhang, P., Hetherington, C. J., Gonzalez, D. A., Zhang, D. E., Moreau-Gachelin, F., & Tenen, D. G. (1995). PU.1 (Spi-1) autoregulates its expression in myeloid cells. *Oncogene*, *11*, 1549–1560.
18. Yang, C., Tao, H., Zhang, H., Xia, Y., Bai, J., Ge, G., Li, W., Zhang, W., Xiao, L., Xu, Y., Wang, Z., Gu, Y., Yang, H., Liu, Y., & Geng, D. (2022). TET2 regulates osteoclastogenesis by modulating autophagy in OVX-induced bone loss. *Autophagy*, *18*, 2817–2829. https://doi.org/10.1080/15548627.2022.2048432.
19. Vidoni, C., Follo, C., Savino, M., Melone, M. A., & Isidoro, C. (2016). The role of cathepsin D in the pathogenesis of human neurodegenerative disorders. *Medicinal Research Reviews*, *36*, 845–870. https://doi.org/10.1002/med.21394.
20. Aghdassi, A. A., John, D. S., Sendler, M., Weiss, F. U., Reinheckel, T., Mayerle, J., & Lerch, M. M. (2018). Cathepsin D regulates cathepsin B activation and disease severity predominantly in inflammatory cells during experimental pancreatitis. *J Biol Chem*, *293*, 1018–1029. https://doi.org/10.1074/jbc.M117.814772.
21. Deng, Y. X., He, W. G., Cai, H. J., Jiang, J. H., Yang, Y. Y., Dan, Y. R., Luo, H. H., Du, Y., Chen, L., & He, B. C. (2021). Analysis and validation of hub genes in blood monocytes of postmenopausal osteoporosis patients. *Frontiers in Endocrinology*, *12*, 815245. https://doi.org/10.3389/fendo.2021.815245.
22. Hwang, J. H., Park, Y. S., Kim, H. S., Kim, D. H., Lee, S. H., Lee, C. H., Lee, S. H., Kim, J. E., Lee, S., Kim, H. M., Kim, H. W., Kim, J., Seo, W., Kwon, H. J., Song, B. J., Kim, D. K., Baek, M. C., & Cho, Y. E. (2023). Yam-derived exosome-like nanovesicles stimulate osteoblast formation and prevent osteoporosis in mice. *Journal of Controlled Release*, *355*, 184–198. https://doi.org/10.1016/j.jconrel.2023.01.071.
23. Wang, X., Chen, T., Deng, Z., Gao, W., Liang, T., Qiu, X., Gao, B., Wu, Z., Qiu, J., Zhu, Y., Chen, Y., Liang, Z., Zhou, H., Xu, C., Liang, A., Su, P., Peng, Y., & Huang, D. (2021). Melatonin promotes bone marrow mesenchymal stem cell osteogenic differentiation and prevents osteoporosis development through modulating circ_0003865 that sponges miR-3653-3p. *Stem Cell Research & Therapy*, *12*, 150. https://doi.org/10.1186/s13287-021-02224-w.
24. Serigano, K., Sakai, D., Hiyama, A., Tamura, F., Tanaka, M., & Mochida, J. (2010). Effect of cell number on mesenchymal stem cell transplantation in a canine disc degeneration model. *Journal of Orthopaedic Research*, *28*, 1267–1275. https://doi.org/10.1002/jor.21147.
25. Yang, N., Zhang, X., Li, L., Xu, T., Li, M., Zhao, Q., ... & Liu, Z. (2022). Ginsenoside Rc promotes bone formation in ovariectomy-induced osteoporosis in vivo and osteogenic differentiation in vitro. *International Journal of Molecular Sciences,* 23, https://doi.org/10.3390/ijms23116187.
26. Tella, S. H., & Gallagher, J. C. (2014). Prevention and treatment of postmenopausal osteoporosis. *The Journal of Steroid Biochemistry and Molecular Biology*, *142*, 155–170. https://doi.org/10.1016/j.jsbmb.2013.09.008.
27. Hattner, R., Epker, B. N., & Frost, H. M. (1965). Suggested sequential mode of control of changes in cell behaviour in adult bone remodelling. *Nature*, *206*, 489–490. https://doi.org/10.1038/206489a0.
28. Eriksen, E. F. (1986). Normal and pathological remodeling of human trabecular bone: Three dimensional reconstruction of the remodeling sequence in normals and in metabolic bone disease. *Endocrine Reviews*, *7*, 379–408. https://doi.org/10.1210/edrv-7-4-379.
29. Lane, N. E. (2006). Epidemiology, etiology, and diagnosis of osteoporosis. *American Journal of Obstetrics and Gynecology*, *194*, S3–S11. https://doi.org/10.1016/j.ajog.2005.08.047.
30. Cuadrado, A., & Nebreda, A. R. (2010). Mechanisms and functions of p38 MAPK signalling. *Biochemical Journal*, *429*, 403–417. https://doi.org/10.1042/BJ20100323.
31. Williams, L. M., & Gilmore, T. D. (2020). Looking down on NF-kappaB. *Molecular and Cellular Biology,* 40, https://doi.org/10.1128/MCB.00104-20.
32. Glick, D., Barth, S., & Macleod, K. F. (2010). Autophagy: cellular and molecular mechanisms. *J Pathol*, *221*, 3–12. https://doi.org/10.1002/path.2697.
33. Xu, X., Lai, Y., & Hua, Z. C. (2019). Apoptosis and apoptotic body: disease message and therapeutic target potentials. *Bioscience Reports,* 39, https://doi.org/10.1042/BSR20180992.
34. Boivin, G., Farlay, D., Bala, Y., Doublier, A., Meunier, P. J., & Delmas, P. D. (2009). Influence of remodeling on the mineralization of bone tissue. *Osteoporosis International*, *20*, 1023–1026. https://doi.org/10.1007/s00198-009-0861-x.
35. Khosla, S., & Shane, E. (2016). A crisis in the treatment of osteoporosis. *Journal of Bone Mineral Research*, *31*, 1485–1487. https://doi.org/10.1002/jbmr.2888.